# Online Wavelet Complementary Velocity Estimator

Paolo Righettini[a], Roberto Strada[a], Ehsan KhademOlama[a,*], Shirin Valilou[a]

[a] *Università degli studi di Bergamo,*
*Department of Engineering and Applied Sciences,*
*Mechatronics Laboratory*

**Abstract**

In this paper, we have proposed a new online Wavelet Complementary velocity Estimator (WCE) over position and acceleration data gathered from an electro hydraulic servo shaking table. This is a batch estimator type that is based on the wavelet filter banks which extract the high and low resolution of data. The proposed complementary estimator combines these two resolutions of velocities which acquired from numerical differentiation and integration of the position and acceleration sensors by considering a fixed moving horizon window as input to wavelet filter. Because of using wavelet filters, it can be implemented in a parallel procedure. By this method the numerical velocity is estimated without having high noise of differentiators, integration drifting bias and with less delay which is suitable for active vibration control in high precision Mechatronics systems by Direct Velocity Feedback (DVF) methods. This method allows us to make velocity sensors with less mechanically moving parts which makes it suitable for fast miniature structures. We have compared this method with Kalman and Butterworth filters over stability, delay and benchmarked them by their long time velocity integration for getting back the initial position data.

*Keywords:* Wavelet Filter Banks, Complementary Filter, Velocity Estimation, Sensor Integration, Data Fusion, Intelligent Sensors, State Estimation.

*Corresponding author
*Email addresses:* paolo.righettini@unibg.it (Paolo Righettini), roberto.strada@unibg.it (Roberto Strada), ehsan.khademolama@unibg.it (Ehsan KhademOlama), shirin.valilou@unibg.it (Shirin Valilou)

## 1. Introduction

High speed in manufacturing of high precision components [1, 2] and micro-feeding Mechatronics solutions, is a prime requirement. The main problem of mass production of the precise components is their high price of machinery tools and the time consumption in the production processes. To being precise, it needs high quality in surfacing and dimensioning in the production line. For precise producing goods, todays mechanical structures in analysis and production parts has been reached to the highest levels in decades. But, what mainly effects the precision in the machinery tools, is the vibration induced to the mechanical structures from various sources such as natural frequencies of the working structure in higher speeds and oscillations induced by nonlinear frictions in lower speeds [3]. In heavy duty operations like steel face milling the critical modes for vibration are related to the whole machine tool structure (chatter frequency is between 15 and 100Hz). The introduction of additional damping in the machine tool structure can increase milling stability. However, a passive absorber is not feasible in many machining processes where the dynamics of the system change according to the working position and an active damper is needed. The famous Direct Velocity Feedback (DVF) are well known in active suspension literature [4, 5, 6, 7] from old to new methods such as sky-hook [8, 9]. The DVF, which utilizes actuators and the acceleration signal from sensor, is an advanced Mechatronics solution which in performance is comparable with smart materials like piezoelectric actuators in damping strategies. This solution is cheaper in cost, but its reliability is strictly challenged by inner algorithms for sensor fusion and controller types. Any good controller has a bandwidth which is limited by its sensory inputs. So using high quality sensor feedback to controller maximizes the whole control system bandwidth. Designing soft sensors to deriving high quality velocity from other sensors in real time due to the technical difficulties is an open challenge in literature[10].

Traditional inertial velocity sensors are based on the movement of a mechanical mass in an electromagnetic field which produces some currents to be

sensed. Otherwise piezoelectric velocity sensors are accelerometers with an electronic integrator built in to the unit with a high pass filter for removing the bias created by integrator [11]. So deriving this velocity from online numerical differentiation or integration of a measured data with noises has great importance in signal processing, control engineering [12, 13, 14], numerical analysis, or failure diagnostics [15]. It is used in implementation of control strategies which uses the least cost sensors available (just position or angular). But, these low cost sensors deliver such a noise over useful signal which using numerical differentiators over them gives a high noisy results which is practically unusable in high precision works and must use some kinds of filter where each of these filters have their own benefits and problems.

Different online linear filters such as Butterworth or Chebyshev Types I and II, elliptic and some nonlinear filters such as wavelet [16, 17] have been used in the industry for removing this kind of noise from digital differentiators. Another approach is based on the least square on a polynomial structure [18, 19]. High gain observers which adjust the model by weighting the observer output deviations from the system to be controlled [20, 21] is another implementation. Design of numerical differentiators in the frequency domain is based on the assumption that an ideal $n-th$ order differentiator has a frequency response of magnitude $\omega^n$ [22, 23, 24]. Extended Kalman Filter is a special strategy for state estimation which can be used for digital differentiation [25, 26, 27]. The main problem in differentiator design is to combine differentiation exactness with robustness in respect to possible measurement errors and input noises. But most of these filters have delays because of deleting high frequency contents of the signal and phase shifting in much frequencies. If nothing is known on the signal structure except some differential inequalities, then sliding modes [28, 29] for its exactness and robustness are used. This method is good as the noise on the signal is as low as possible, with high noise the differentiator results contains a high chattering which makes it impossible use in real feedback control systems. A simple and old estimation technique for velocity that is often used in the flight control industry is to fusion measurements in the complementary filter [30]. A

complete overview on all these filters has been done in [31].

The Wavelet Transform (WT) is a powerful tool of signal and image processing and it has been vastly used in many scientific areas, such as signal processing, image compression, computer graphics, and pattern recognition [32, 33, 34, 35, 36]. Noise filtering using wavelet has been a very mature technology [37, 38, 39]. On contrary the traditional Fourier Transform, the WT is particularly suitable for the applications of non-stationary signals which may instantaneous vary in time [40, 41]. But even the wavelet filtering alone on a specific signal, based on its nature tries to remove(or smoothen) the higher resolutions beneath the original signal, so it causes delay in output filtered signal. Many attempts have been done in joining wavelet multi-resolution analysis with kalman filtering to estimate states from high noise data [42, 43, 44, 45]. These methods require application of kalman filter over each resolution level, which needs high serially computation resources.

So, finding fast and accurate algorithms which could give the absolute velocity value of the system with low noise, least delay and stable properties, is the main challenge of this paper. This fast and reliable velocity can give us high precision accuracy out of control feedbacks regardless of environmental vibrations.

At this paper, in the next section we define the mathematical definitions needed for presenting the position, velocity and the acceleration with some preliminaries on discrete wavelet, Butterworth for noise canceling and Kalman filter for state estimation have been introduced. In the third section, structure of the proposed complementary estimator is mathematically explained and proved. The fourth section describes the experimental results in compare to kalman filter, the butterworth and a complementary estimator which uses butterworth filters instead of wavelets.

## 2. Problem Definition and Preliminaries

By considering an analog position signal as $P_s(t)$ and an analog acceleration signal as $A_s(t)$ we can construct an object motion states as:

$$\begin{aligned} \begin{bmatrix} P_r' \\ V_r' \\ A_r' \end{bmatrix} &= \begin{bmatrix} 0 & 1 & 0 \\ 0 & 0 & 1 \\ 0 & 0 & 0 \end{bmatrix} \begin{bmatrix} P_r \\ V_r \\ A_r \end{bmatrix} + w \\ \begin{bmatrix} P_s \\ A_s \end{bmatrix} &= \begin{bmatrix} 1 & 0 & 0 \\ 0 & 0 & 1 \end{bmatrix} \begin{bmatrix} P_r \\ V_r \\ A_r \end{bmatrix} + v \end{aligned} \tag{1}$$

Where the states are $X(t) = [P_r(t), V_r(t), A_r(t)]'$ and sensed data are $Y(t) = [P_s(t), A_s(t)]'$. The $w = N(0, Q)$ and $v = N(0, R)$ are the uncertainties with Gaussian Distribution of variances $Q$ and $R$. The goal of this paper is to estimating $V_r(t)$ with lowest delay as possible. In contrary to lowest delay, we also want to acquire a velocity which is suitable for stabilizing control feedbacks which contains integration procedures inside.

### *2.1. Multi-Resolution Analysis and Discrete Wavelet Transform*

Multiresolution Analysis (MRA) is a convenient framework for hierarchical representation of functions or signals on different scales. The basic idea of multiresolution analysis is to represent a function $f(x)$ as a limit of successive approximations. Each of these successive approximations is a smoother version of the original function with more and more of the finer "details" added. Wavelets are terminating basis vectors which are used to decompose a signal using a set of coefficients. The process of decomposition uses a sub-band coding scheme that is illustrated in Fig.1. The Discrete Wavelet Transform (DWT) can be computed using the filter banks $\overline{h(k)}$ and $\overline{g(k)}$ which form a quadrature conjugate mirror filter pair with $h(k)$ and $g(k)$, which are given by Eqs.A.7 from two conjugate functions, the wavelet function $\psi(x)$ and the scaling function $\phi(x)$. The result of the analysis step is a set of intermediate coefficients, which represent the weights of the original signal in terms of the basis functions used,

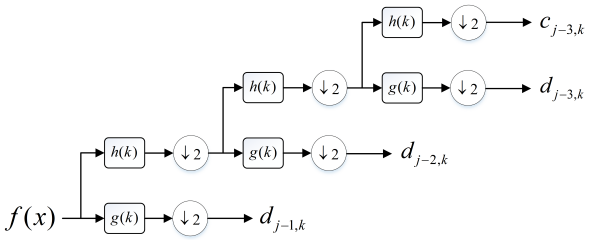


Figure 1: Illustration of the analysis part of a three-level decomposition scheme using sub-band coding.

namely the scaling function and the wavelet function. The original sampled signal is filtered with the scaling function and the wavelet function and down sampled by two, resulting in the trend and detail coefficients at level one. The trend coefficients thus obtained are then used as the original signal and filtered with the scaling function and the wavelet to yield the coefficients at level two. This process is repeated depending upon the number of decomposition levels desired. For reverse procedure, the detail and the scale add up, then being up-sampled and passed from reverse scale filter, ready to being added to detail of the lower levels. By these coefficients the $f(x)$ can be decomposed in wavelet and scale spaces as equations A.6.

The problems of temporal and frequency resolution found in the analysis of signals with the Short time Fourier Transform (STFT), i.e. best resolution in time at the expense of a lower resolution in frequency and vice-versa, can be reduced through the MRA provided by Discrete Wavelet Transform (DWT). The temporal resolutions, $\Delta t$, and frequency, $\Delta f$, indicate the precision time and frequency in the analysis of the signal. Both parameters vary in terms of time and frequency, respectively, in signal analysis using DWT. Unlike the STFT, where a higher temporal resolution could be achieved at the expense of frequency resolution. Intuitively, when the analysis is done from the point of view of filters series, the temporal resolution should increase increasing the center frequency of the filters bank. Thus, $\Delta f$ is proportional to $f$. The main difference between DWT and STFT is the time-scaling parameter. The result

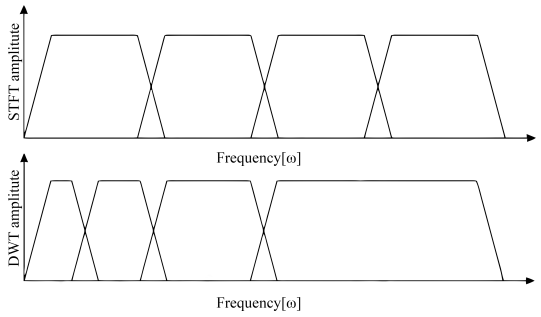


Figure 2: Comparison between STFT and DWT in their frequency domain signal decomposition.

is geometric scaling that gives the DWT logarithmic frequency coverage with nonlinear phase distortion in contrast to the uniform frequency coverage of the STFT, as compared in Fig.2.

### *2.2. Butterworth Filter*

The Butterworth filter is a type of signal processing filter designed to have as flat a frequency response as possible in the passband. It is also referred to as a maximally flat magnitude filter. In [46, 47] design procedures has been described. For selection of an optimal cutoff frequency and order has been discussed in [48, 49] exhaustively. But for precision, it has been developed a pattern search optimization method which finds the optimal cutoff frequency and order with comparison of the filter output to offline computed velocity data. These velocity data has been processed by a non casual offline smooth differentiation from position data in 512 sampling windows. The optimal cutoff frequency found for our system is $30[Hz]$ frequency with the order of 2 by a delay of $7[ms]$ in the output. In Fig.3, use of this filter after a direct differentiator has been shown. As it is obvious there is a delay in results which makes this filter unreliable in high precision-high speed processes.

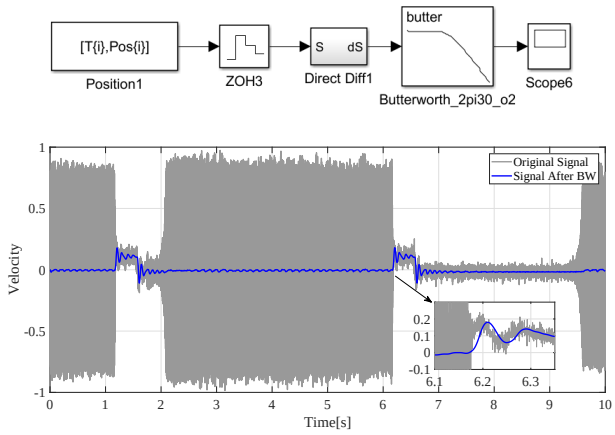


Figure 3: Numerical Differentiator followed by a butterworth filter.

### *2.3. Kalman Filter*

Kalman filter is the most famous for estimation of system states by fusion of the noisy input signals [50]. In this paper for comparison we have considered a tri-state system differentiator which has been derived by discretization of the continuous object motion states:

$$\begin{aligned}
\overbrace{\begin{bmatrix} P(k+1) \\ V(k+1) \\ A(k+1) \end{bmatrix}}^{X(k+1)} &= \overbrace{\begin{bmatrix} 1 & \Delta t & \frac{\Delta t^2}{2} \\ 0 & 1 & \Delta t \\ 0 & 0 & 1 \end{bmatrix}}^{\Gamma} \overbrace{\begin{bmatrix} P(k) \\ V(k) \\ A(k) \end{bmatrix}}^{X(k)} + w \\
\overbrace{\begin{bmatrix} P_s(k) \\ A_s(k) \end{bmatrix}}^{Y(k)} &= \overbrace{\begin{bmatrix} 1 & 0 & 0 \\ 0 & 0 & 1 \end{bmatrix}}^{C} \begin{bmatrix} P(k) \\ V(k) \\ A(k) \end{bmatrix} + v
\end{aligned} \tag{2}$$

Where the discrete states are $X(k) = [P(k), V(k), A(k)]'$ and sensed data are $Y(k) = [P_s(k), A_s(k)]'$ by considering sample time $\Delta t$. The $w = N(0, Q)$ and $v = N(0, R)$ are the uncertainties with Gaussian Distribution of variances $Q$ and $R$. Kalman filter has a two-step procedure for state estimation. In the prediction step, The current state and error noise covariances are used to project forward through the state model in order to estimate the predicted mean and covariances. This is called as the a priori estimate. Once the outcome of the

next measurement (corrupted with random noise) is observed, these estimates are updated using a weighted average, with more weight being given to estimates with higher certainty. These two steps equations for our differentiator case are as follows:

- Initialization: It consists of choosing good initials for $X_{k-1}^{-}$ and $P_{k-1}^{-}$
- Prediction:

$$\begin{aligned} \hat{X}_k^- &= \Gamma \hat{X}_{k-1} \\ P_k^- &= \Gamma P_{k-1} \Gamma^T + Q \end{aligned} \tag{3}$$

- Update:

$$\begin{aligned} K_k &= P_k^- C^T (C P_k^- C^T + R)^{-1} \\ \hat{X}_k &= \hat{X}_k^- + K_k (Y - C \hat{X}_k^-) \\ P_k &= (I - K_k C) P_k^- \end{aligned} \tag{4}$$

The algorithm is recursive. It can run in real time, using only the present input measurements and the previously calculated state and its uncertainty matrix, so no additional past information is required.

### *2.4. Complementary Filters*

Complementary Filter (CF) scheme is used wildly in many areas of digital technology we have, from aerospace [51, 30] to mobile tracking devices [52]. This filter is actually a steady state Kalman filter (i.e., a Wiener filter) for a certain class of filtering problems[30]. A complementary Filter shown in Fig.4 consists of two or more filters, which in together produce one output from multi-input, where each filter choose to give one part of the output based on the space which the filters are complementary in. This configuration shows how a low pass filter $G(s)$ can remove high frequency noise $n_2$ and low frequency disturbance $n_1$ from variable $X$. Traditionally CFs, shown in Fig.5 has been used in finding tilte angle of Mechatronics or UAVs in an accurate low noise signal from accelerometer and gyroscope [53, 54].

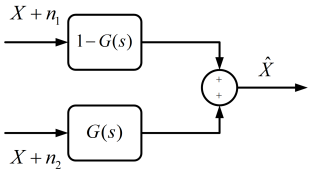


Figure 4: Complementary filter scheme.

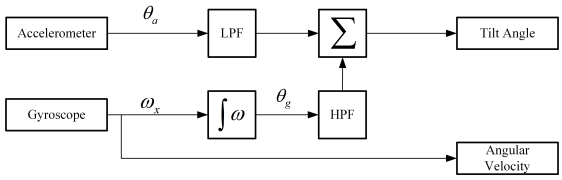


Figure 5: Traditional complementary filter for estimating title from accelerometer and gyroscope.

### *2.5. Delay Analysis of Complementary Filters*

All the complementary filters use simple properties of All-Pass band Filters[55] (APF). In an APF we have two or more filters which the summation of their gain is unity with kernel based phase delay and with their group delay could change the behavior of the signal[56]. Group delay denoted by $\tau_g(\omega)$ vs Phase delay denoted by $\tau_p(\omega)$ is the time delay of the amplitude envelopes of the various sinusoidal components of a signal through a device under test, and is a function of frequency for each component. Phase delay, in contrast, is the time delay of the phase as opposed to the time delay of the amplitude envelope. If the filter's transfer function is $H(j\omega)$, then we have:

$$\begin{aligned} \phi(\omega) &= \arg\{H(j\omega)\} \\ \tau_g(\omega) &= -\frac{d\phi(\omega)}{d\omega} \\ \tau_p(\omega) &= -\frac{\phi(\omega)}{\omega} \end{aligned} \tag{5}$$

The complementary filter can be reconfigured as in Fig.6 from Fig.4. In this case the input to $G(s)$ is $n_2 - n_1$, so that the filter $G(s)$ just operates on the noise and the original variable $X$ flows out by the delay configured according to the unity APF phase. For illustration in Fig.7 the group delay of a butterworth filter

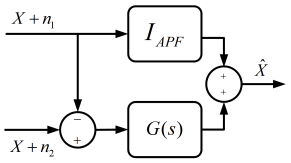


Figure 6: Reconfigured complementary filter, which shows the Unity all-pass filter affect on the estimated variable.

and Haar wavelet($1th$ order) has been shown. As it is obvious the Haar wavelet group delay is just half a sample which is high better than the butterworth nonlinear with high samples of delay.

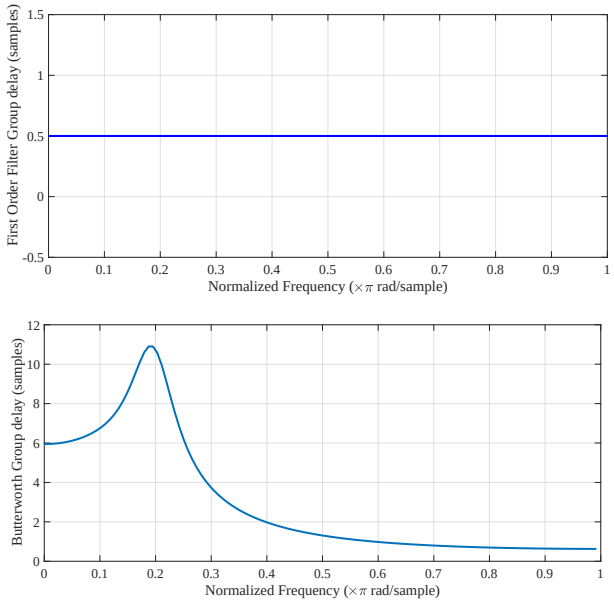


Figure 7: The group delay of butterworth filter shows a nonlinear behavior with high peak of $11[samples]$ around $0.2 \times \pi/sample$, in contrary Haar wavelet($1th$ order) has a very low (0.5[Sample]) of group delay.

## 3. Wavelet Complementary Estimator

As shown in Fig.8 and Fig.9, We have designed a moving horizon complementary filter in which two wavelet filters produce one output velocity data from two sources. The first source comes from differentiating of position sensor and the second one comes from integrating of acceleration data. If we consider position and acceleration as:

$$\begin{aligned} P(k) &= P_r(\Delta t \times k) + N_p(0, \sigma_p) \\ A(k) &= A_r(\Delta t \times k) + N_a(0, \sigma_a) \end{aligned} \tag{6}$$

where $P(k)$ and $A(k)$ are sample of position and acceleration from continuous $P_r$ and $A_r$ with sample time of $\Delta t$. These two signals carry white noises with covariances $\sigma_p$ and $\sigma_a$. Now if we take numerical derivative from $P(k)$ and numerical integration from $A(k)$ we get two numerical representation of real velocity $V(n)$ as:

$$\begin{aligned} V_d(n) &= V(n - d_d) + \tfrac{\Delta N_p(0,\sigma_p)}{\Delta t} \\ V_i(n) &= V(n - d_i) + b_0 n + \textstyle\sum N_a(0, \sigma_a) \end{aligned} \tag{7}$$

where $d_d$ and $d_i$ are the delay produced by numerical operators, differentiation and integration respectively. The first one consists of violet noise (Differentiation of white noise), but without any drift in output and the second one is a good velocity data but having bias $b_0$ came from numerical integration procedure on initial mean value of acceleration and local mean of discrete white noise and a brown(ian) noise (Integration of white noise).

### *3.1. Mathematical Definition*

As said in introduction, wavelet filters alone removes data from signals. But here by combining two higher and lower resolutions data from two relevant signal we get almost all data back. If we consider the delays from operators could be neglected, we can derive the discrete wavelet transform of both velocities by

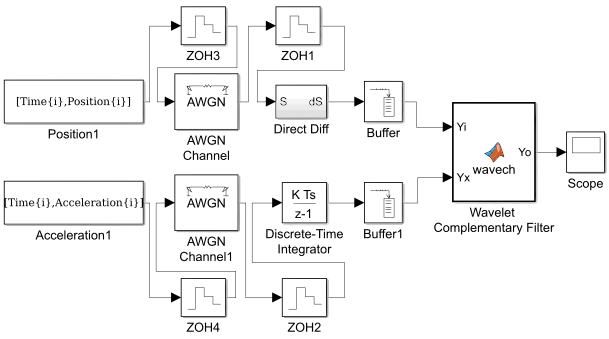


Figure 8: Scheme of the Wavelet Complementary Velocity Estimator which is consists of two parts. the upper part is numerical differentiator and the lower part is the numerical integrator.

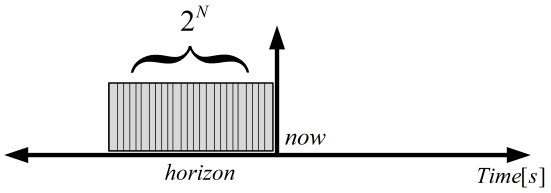


Figure 9: Moving Horizon of the Wavelet Complementary Estimator which is consists of $2^N$ buffered samples.

using appendix A equations for data length of $2^N$ as:

$$\begin{aligned}
{c^d}_{N,k} &= \sum_k \{V(n) + N_{violet}(0,\sigma)\}\overline{\phi_{N,k}(n)} \\
{d^d}_{m,k} &= \sum_k \{V(n) + N_{violet}(0,\sigma)\}\overline{\psi_{m,k}(n)} \\
{c^i}_{N,k} &= \sum_k \{V(n) + b_0 n + N_{brown}(0,\sigma)\}\overline{\phi_{N,k}(n)} \\
{d^i}_{m,k} &= \sum_k \{V(n) + b_0 n + N_{brown}(0,\sigma)\}\overline{\psi_{m,k}(n)}
\end{aligned} \tag{8}$$

As the function $\{N_{violet}(0,\sigma)\}\overline{\phi_{N,k}(n)}$ is an even function and $\{b_0 n\}\overline{\psi_{m,k}(n)}$ is an odd function over large $k$ we can expect that the following summations goes to zero:

$$\begin{aligned}
C &= \sum_k \{N_{violet}(0,\sigma)\}\overline{\phi_{N,k}(n)} \approx 0 \\
D &= \sum_k \{b_0 n + \overbrace{N_{brown}(0,\sigma)}^{\approx 0}\}\overline{\psi_{m,k}(n)} \approx 0
\end{aligned} \tag{9}$$

We have constructed our new complementary filter by choosing the filter coefficients as:

$$
\begin{aligned}
& f^{c}(x) = \sum_{k} {c^{c}}_{N,k}\phi_{N,k}(x) + \sum_{m=1}^{N}\sum_{k} {d^{c}}_{m,k}\psi_{m,k}(x) \\
& {c^{c}}_{N,k} = {c^{d}}_{N,k} \\
& {d^{c}}_{m,k} = {d^{i}}_{m,k}
\end{aligned}
\tag{10}
$$

This gives us a results with much less bias and noise. In addition based on the structure we can connect this estimator concurrently in serially manner.

### *3.2. WCE Delay Analysis*

One of the main characteristics of the wavelet filter banks is their lossless reconstruction of the data from converted data through filter banks[57] if the processing frequency is greater than sampling frequency. This feature comes from recursive algorithms which wavelet's kernels are based on. In contrary to Fig.6 that there is just an APF with nonlinear phase and group delay in the middle of the input and output signal, the WCE uses an APF in each sub down resolution. This procedure is shown in Fig.10. Based on Eq.10 it can be seen that the first source $(S1)$ in the $(N-j)^{th}$ level is added to the second source $(S2)$ in the same level through a low pass filter $\uparrow \Phi'_{N-j-1}(\omega)$ which is consisted of a high sampler and low pass filter of scale wavelet function to $(N-j-1)^{th}$ level, and this procedure continues up to level 0. $I(\omega)$ is the APF and the same for our Haar wavelet kernel based WCE at each resolution.

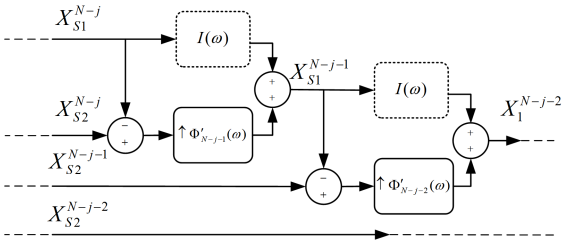


Figure 10: The wavelet complementary procedure involves a unity filter and wavelet low pass filter at each sub-resolution.

As it is said before the complementary structure of the wavelet filter banks allow them to lossless reconstruction of the data which shows their APF structure as unity in gain and zero in phase delay. This is easy to show in our selected Haar kernel. The Haar wavelet filter bank is consisted of two level decomposition, scale and details. It can be written as:

$$\begin{aligned} x^c_{j-1}[n] &= (x^c_j[2n] + x^c_j[2n-1])/\sqrt{2} \\ x^d_{j-1}[n] &= (x^c_j[2n] - x^c_j[2n-1])/\sqrt{2} \end{aligned} \tag{11}$$

If we define $x^c_{j-1}[n]$ as $y$, $x^d_{j-1}[n]$ as $z$, and $2n$ as $k$, we can write upper equations as:

$$\begin{aligned} y &= (x^c_j[k] + x^c_j[k-1])/\sqrt{2} \\ z &= (x^c_j[k] - x^c_j[k-1])/\sqrt{2} \end{aligned} \tag{12}$$

which indicates that, the Haar wavelet filter bank operates as a simple first order low pass and a first order high pass filters for its immediate lower resolution. The fourier transform of Eqs.12 is as:

$$\begin{aligned} Y(\omega) &= X^c_j(\omega)(1 + e^{-i\omega}) \times \sqrt{2} \\ Z(\omega) &= X^c_j(\omega)(1 - e^{-i\omega}) \times \sqrt{2} \end{aligned} \tag{13}$$

By adding these two simple equations together to construct an APF for that resolution we can go back to original estimated lower resolution. This characteristic shows why we can reconstruct lower resolutions from higher ones without losing data or phase and group delay (if processing frequency is higher than sampling).

## 4. Results and Discussions

For illustrating the power of this filter we tried two basket of data. One is the artificial sinusoidal function with white Gaussian noise over them to benchmark it with other methods and the other is some collected position and acceleration data from a real shaking table shown in Fig.11. The shaking table is activated by various input voltage signals, where here in this article we have used the step function input as case study. The position and acceleration measurements of

the system are carried out by linear potentiometer transducer PC-M-300) and accelerometer (ADXL05EM-EM-3) separately. Every measurement is recorded with the sampling frequency of $2K[Sps]$, which is shown in Fig.12. The

Figure 11: Physical shaking table in our laboratory.

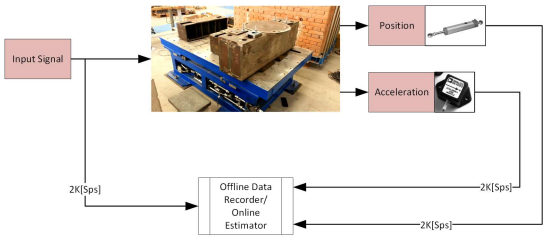


Figure 12: Structure of data gathering system.

sinusoidal function, shown in Fig.13 are:

$$\begin{cases} S = 10\sin(2\pi t) + N(0, \sigma_1) \\ \frac{dS}{dt} = 20\pi\cos(2\pi t) \\ \frac{d^2S}{dt^2} = -40\pi^2\sin(2\pi t) + N(0, \sigma_2) \end{cases} \tag{14}$$

In the simulation case, the position sensor Signal to Noise Ration (SNR) is set to $70[dB]$ and the acceleration sensor SNR is set to $10[dB]$. The Fig.14 shows comparison between butterworth and our estimator. The WCE results have almost no delay with respect to butterworth filter in spite of more digestible noise over it. As it is clear the WCE takes more time to converges to the real velocity. The next comparison is with the Kalaman Filter, which has been

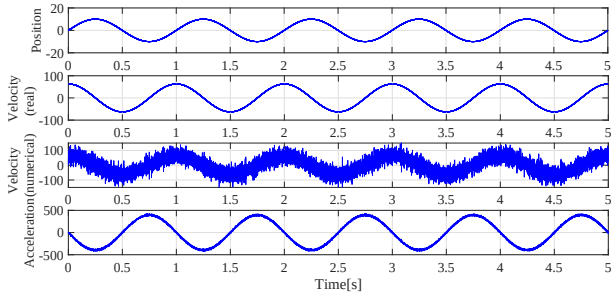


Figure 13: Sinusoidal Position, Real Velocity, Velocity from numerical differentiation and Acceleration for benchmarking the Wavelet Complementary Estimator.

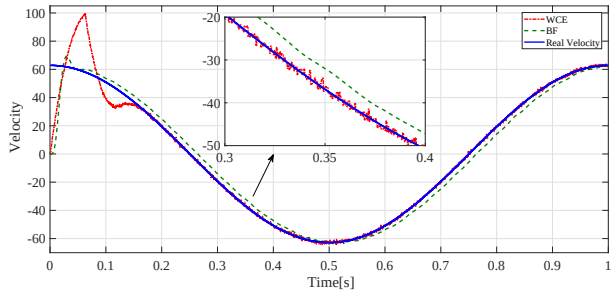


Figure 14: Comparison of Wavelet Complementary Estimator with butterworth filter, it shows the delay conventional filters.

shown in Fig.15. Kalman Filter after 3 seconds has been successfully converged to the real velocity. This result is comparable to next simulation of kalman filter which could not converge to real velocity, which proposes that the kalman filter is just applicable in data sets which has no bias. Besides our complementary estimator, we have designed an Ordinary Complementary Estimator (OCE) that uses traditional butterworth filters, one highpass for integration part and one lowpass for differentiation part, instead of our wavelet filter banks. The results are shown in Fig.16. For benchmarking the WCE, we have considered the long term ($10[s]$) velocity integration to compare it with real position. This test bench shows how much the data produced can be trustable for producing

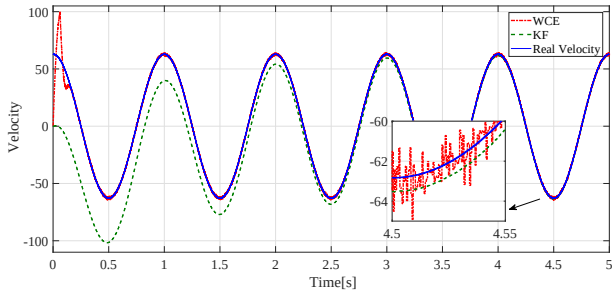


Figure 15: Comparison between the Kalman Filter and WCE which shows WCE's faster convergences, but kalman filter's better results in non biased data sets.

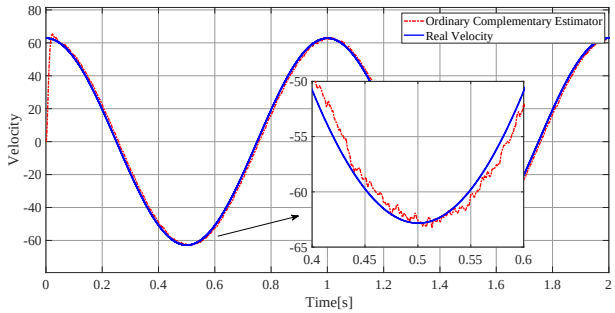


Figure 16: Results of the ordinary complementary estimator shows a stable, fast converging but biased output.

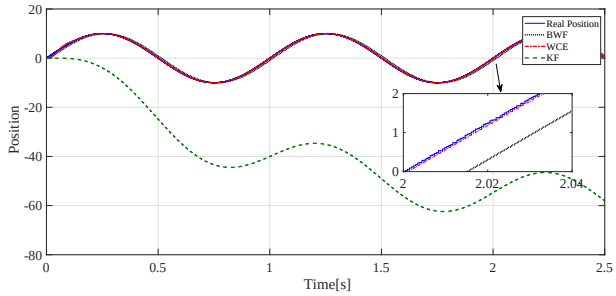


Figure 17: Integration benchmark for Kalman and Butterworth filters and the WCE. Kalman Filter goes off and the other two stays with real position data.

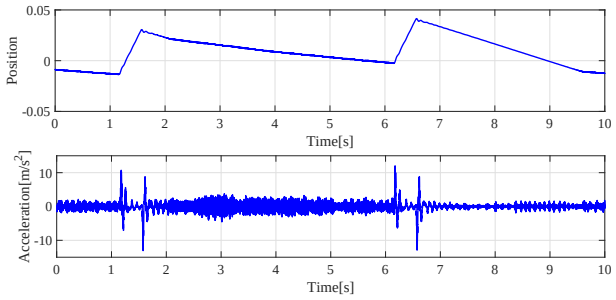


Figure 18: Position and Acceleration gathered from sensors.

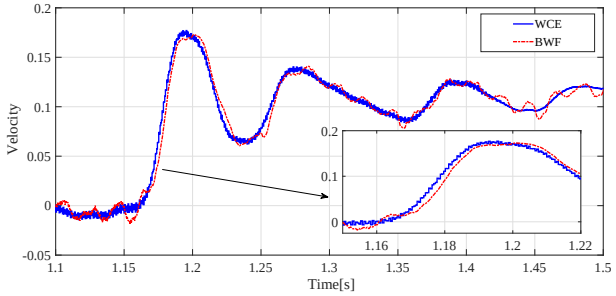


Figure 19: Velocity estimation by Wavelet Complementary and Butterworth $2\pi 60(rad)order2$ Filters.

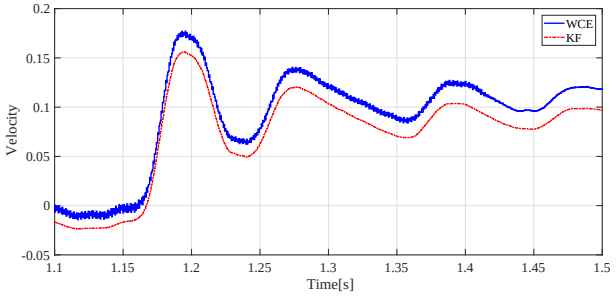


Figure 20: Velocity estimation by Wavelet Complementary and Kalman filters.

stable control outputs in feedback systems. Fig.17 shows the integration results. Integration of the Kalman Filter goes wild off the road, but butterworth and

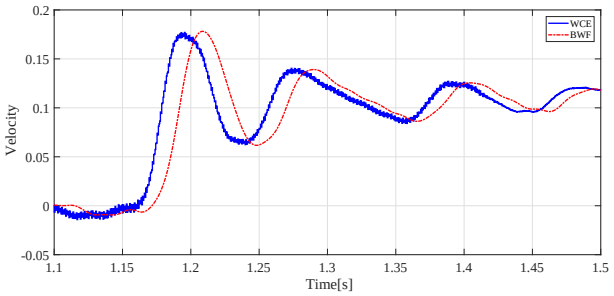


Figure 21: Comparing velocity estimation with Butterworth filtering $2\pi 30(rad)order4$ after numerical differentiator.

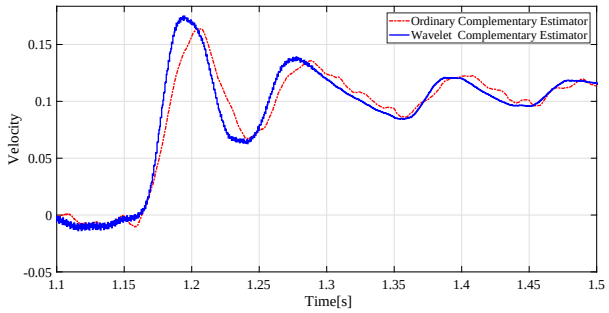


Figure 22: Velocity estimation by Wavelet Complementary and Ordinary Complementary with butterworth $2\pi 30(rad)order2$ Filters.

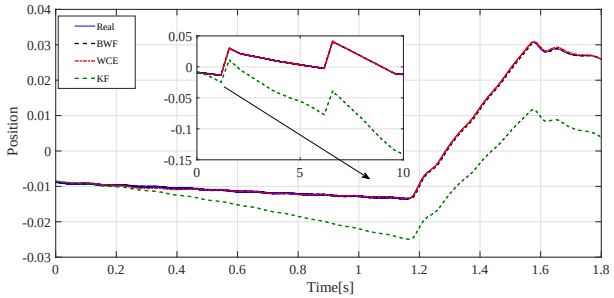


Figure 23: Position from velocity integration of filters to comparison, as seen kalman filter has a large bias in this benchmark.

Table 1: Mean Square Error comparison of four filters in Velocity and Position from long integration for sinusoidal signal.

| | WCE | KalmanF | BWF | OCE |
|---|---|---|---|---|
| MSE[Vel] | 3.629 | 100.003 | $1.974\times10^3$ | 5.925 |
| MSE[IPos] | 0.002 | $3.701\times10^3$ | 0.3314 | 0.126 |

the WCE stays in stable manner. As it is obvious, WCE has no delay with compare to the butterworth filter.

For better comparison the Mean Square Error of the results has been tabled in the table.1. In the Fig.18, a gathered data set of the position and acceleration is shown. We try to estimate the velocity of system based on these two gathered data. In a control feedback, usually we need a stable and clean data to compensate the disturbances in output. So, removing delay and stabilization are the most important goals of any state estimators. Here in Figs.19-22, we have compared the velocity results of the four methods, Butterworths, Kalman Filter and Wavelet Complementary Estimator with real data. The butterworth filter has order 2 with cutoff frequency of $60[Hz]$. The moving horizon width of the Wavelet Complementary Estimator is chosen 256 samples with the Haar wavelet kernel. The results of Fig.19 shows that the butterworth filter even with high cutoff frequency has the delay and oscillation problems. In contrary kalman filter results are much smooth and stable, but with a large bias that is unusable in state feedback nonlinear controllers. For illustration of the stability of the WCE, in Fig.23 the integration of these three filters has been shown which implies the correctness of the WCE beside the conventional buttherworth.

## 5. Conclusions

In this paper we have proposed a simple algorithm with just one parameter of moving horizon windows length to estimate velocity from position and acceleration data for active vibration control of high speed high precision processes. As seen, The proposed Wavelet Complementary velocity Estimator has the best

stability with lowest delay results with respect to butterworth filtering methods and kalman filter estimation, which is achieved by considering just one parameter of filter, the moving horizon window's length. This low delay comes from its low total group delay $0.5[sample]$ with respect to butterworth filter. But the MSE analysis results in table.1 show that the ordinary complementary estimator (OCE) with traditional butterworth kernel has almost similar but with much delay, which provides another scheme for designing whether if such delay is acceptable. Because of its low delay and integration stability, it is much more suitable for using in the online control feedback applications. The main problem for WCE, is the noise in numerical differentiation part. As the noise goes up for finding the low resolution of the filter we have to take more samples as moving windows horizon, which causes more deviation of results from real velocity. This problem can be resolved with considering better numerical differentiator instead of our crude step type. As its nature, the algorithm is suitable for parallelism and can be implemented on an FPGA. The MATLAB simulation and data can be downloaded from:

https://www.mathworks.com/matlabcentral/fileexchange/62831-real-time-wavelet-complementary-velocity-estimator

This simulation reconstruct the online situation in which the algorithm has been established.

## Appendix A. Wavelet Transform

Consider a sampled signal $f(x)$ and generate the following sequence of approximations [58]:

$$\begin{aligned} f^m(x) &= \sum_{n=-\infty}^{\infty} f_{m,n}\phi(2^m x - n)_{m=0,1,2,\dots} \\ f(x) &= \sum_m f^m(x) \end{aligned} \tag{A.1}$$

Each approximation is expressed as the weighted sum of the shifted versions of the same function $\phi(x)$ , which is called the scaling function. If the $(m+1)th$

approximation is required to be a refinement of the $mth$ approximation, then the function $\phi(2^m x)$ should be a linear combination of the basis functions spanning the space of the $(m+1)th$ approximation, i.e.,

$$\phi(2^m x) = \sum_k h(k)\phi(2^{m+1}x - k) \tag{A.2}$$

If $V^{m+1}$ represents the space of all functions spanned by the orthogonal set $\{\phi(2^{m+1}x - k); k \in Z$, the set of integers$\}$ and $V^m$ the space of the coarser functions spanned by the orthogonal set $\{\phi(2^m t - p); p \in Z\}$ , then $V^m \subset V^{m+1}$ . Let:

$$V^{m+1} = V^m \otimes W^m \tag{A.3}$$

Then $W^n$ is the space that contains the information added upon moving from the coarser $f^m(x)$ to the finer $f^{(m+1)}(x)$ representation of the original function $f(t)$ . [58] shows that $W^m$ 's are spaces that are spanned by the orthogonal translates of a single function $\psi(2^m x)$ , thus leading to the following equation:

$$f^{(m+1)}(x) = f^m(x) + \sum_{n=-\infty}^{\infty} f_{m,n}\psi(2^m x - n) \tag{A.4}$$

The function $\psi(x)$ is called a wavelet and is related to the scaling function $\phi(x)$ , through the following relationship:

$$\psi(2^m x) = \sum_k g(k)\phi(2^{m+1}x - k) \tag{A.5}$$

$h(k)$ and $g(k)$ form a conjugate complementary mirror filter pair. Concluding the discussion, a mixed-form $N$-level discrete wavelet series representation of the signal is given by:

$$\begin{aligned} f(x) &= \sum_k c_{N,k}\phi_{N,k}(x) + \sum_{m=1}^{N}\sum_k d_{m,k}\psi_{m,k}(x) \\ c_{N,k} &= \sum_k f(x)\overline{\phi_{N,k}(x)} \\ d_{m,k} &= \sum_k f(x)\overline{\psi_{m,k}(x)} \end{aligned} \tag{A.6}$$

where $\overline{\phi(x)}$ and $\overline{\psi(x)}$ are the conjugate functions respectively. Interestingly, the multiresolution concept, besides being intuitive and useful in practice, forms the basis of a mathematical framework for wavelets. One can decompose a function into a coarse version plus a residual and then iterate this to infinity. If properly

done, this can be used to analyze wavelet schemes and derive the wavelet basis. It can be seen from (6) that a wavelet transform decomposes a signal $f(x)$ into trend $c$ and detail $d$ coefficients . An efficient approach in computing the discrete wavelet transform (DWT) is to use the sub-band coding scheme which uses only the filters $h(k)$ and $g(k)$ , which are found to be:

$$\begin{aligned} h(k) &= \sqrt{2}\sum_x \phi(x)\overline{\phi(2x-k)} \\ g(k) &= \sqrt{2}\sum_x \psi(x)\overline{\psi(2x-k)} \\ g(k) &= (-1)^k\overline{h(-k+1)} \end{aligned} \tag{A.7}$$

Equations (6) and (7) provide a hierarchical and fast scheme for the computation of the wavelet coefficients of a given function.

The DWT of a signal $f(x)$ results in trend ($c$) and detail coefficients ($d$) as given by (6). The first step in signal decomposition consists of computing these trend and detail coefficients. Thereafter, the trend coefficients combined with the scaling function as a basis is used to generate the trend signal [left-hand side of the summation in (6)] and the detail coefficients using the wavelets as a basis are used to generate the detail signals [right-hand side of the summation in (6)]. The trend signal captures the high-scale (low-frequency) information and the detail signal captures the low-scale (high-frequency) information contained in the signal $f(x)$. Depending upon the number of decomposition levels, the end product of a multiresolution decomposition is a set of these signals at different scales (frequencies), as shown in (8), where $f_H$ is the high-scale signal, $f_L$ is the low-scale signal, and $f_{M_i}, i = 1, ..., N-1$, are the medium-scale signals where $N$ is the number of decomposition levels. For example, if a three-level decomposition of error signal is done, it results in one trend signal (low frequency) and three detail signals (high and intermediate frequency). There is redundancy in the trend signal; hence, only one obtained at the last level is chosen. The frequency information of these decomposed signals is approximate since the decomposition process does not use a precise frequency-characterized basis vector such as sines and cosines which are used in Fourier analysis:

$$f(x) = f_H(x) + f_{M_1}(x) + ... + f_{M_{N-1}}(x) + f_L(x) \tag{A.8}$$

## References


[1] V. Jain, Micromanufacturing Processes, CRC Press, 2016.

[2] T. Yamaguchi, M. Hirata, J. C. K. Pang, High-speed precision motion control, CRC press, 2017.

[3] J. Brunetti, F. Massi, A. Saulot, M. Renouf, W. DAmbrogio, System dynamic instabilities induced by sliding contact: A numerical analysis with experimental validation, Mechanical Systems and Signal Processing 58 (2015) 70 – 86. doi:10.1016/j.ymssp.2015.01.006.

[4] A. Cowley, A. Boyle, Active dampers for machine tools, Annals of the CIRP 18 (1) (1970) 213–222.

[5] D. Karnopp, Active damping in road vehicle suspension systems, Vehicle System Dynamics 12 (6) (1983) 291–311.

[6] B. Yan, M. Brennan, S. Elliott, N. Ferguson, Active vibration isolation of a system with a distributed parameter isolator using absolute velocity feedback control, Journal of Sound and Vibration 329 (10) (2010) 1601 – 1614. doi:10.1016/j.jsv.2009.11.023.

[7] M. Zaeh, R. Kleinwort, P. Fagerer, Y. Altintas, Automatic tuning of active vibration control systems using inertial actuators, CIRP Annals-Manufacturing Technology.

[8] A. Tiwari, M. Lathkar, P. Shendge, S. Phadke, Skyhook control for active suspension system of heavy duty vehicles using inertial delay control, in: Power Electronics, Intelligent Control and Energy Systems (ICPEICES), IEEE International Conference on, IEEE, 2016, pp. 1–6.

[9] S. Song, F. Jiang, H. Shi, Y. Peng, Skyhook-based body-seat system preview control for a semi-active suspension tractor, Sensors & Transducers 179 (9) (2014) 60.

[10] W.-H. Zhu, T. Lamarche, Velocity estimation by using position and acceleration sensors, IEEE Transactions on Industrial Electronics 54 (5) (2007) 2706–2715.

[11] M. Gavagni, P. Gardonio, S. J. Elliot, Design and fabrication of a micro-velocity sensor for direct velocity feedback control systems, in: Proc. 6th Int. Symp. Active Noise Vibrat. Control, 2006, pp. 1–16.

[12] Y. Zheng, J. Liu, X. Liu, D. Fang, L. Wu, Adaptive second-order sliding mode control design for a class of nonlinear systems with unknown input, Mathematical Problems in Engineering 2015.

[13] F. Beltran-Carbajal, A. Valderrabano-Gonzalez, J. C. Rosas-Caro, A. Favela-Contreras, An asymptotic differentiation approach of signals in velocity tracking control of dc motors, Electric Power Systems Research 122 (2015) 218–223.

[14] A. Levant, Higher-order sliding modes, differentiation and output-feedback control, International journal of Control 76 (9-10) (2003) 924–941.

[15] A. F. de Loza, J. Cieslak, D. Henry, J. Dávila, A. Zolghadri, Sensor fault diagnosis using a non-homogeneous high-order sliding mode observer with application to a transport aircraft, IET Control Theory & Applications 9 (4) (2015) 598–607.

[16] R. Pandey, Design of wavelet-based differentiator filter, Journal of International Academy Of Physical Sciences 17 (1).

[17] E. K. Olama, S. Valiloo, A fast wavelet denoising method, in: 2011 3rd International Conference on Computer Research and Development, Vol. 1, 2011, pp. 492–494. doi:10.1109/ICCRD.2011.5764065.

[18] T. E. Duncan, P. Mandl, B. Pasik-Duncan, Numerical differentiation and parameter estimation in higher-order linear stochastic systems, IEEE Transactions on Automatic control 41 (4) (1996) 522–532.

[19] S. Ibrir, S. Diop, A numerical procedure for filtering and efficient high-order signal differentiation, International Journal of Applied Mathematics and Computer Science 14 (2) (2004) 201–208.

[20] F. Esfandiari, H. K. Khalil, Output feedback stabilization of fully linearizable systems, International Journal of control 56 (5) (1992) 1007–1037.

[21] N. Boizot, E. Busvelle, J. Sachau, High-gain observers and kalman filtering in hard real-time, in: RTL 9th Workshop, 2007.

[22] Y. Chen, B. M. Vinagre, A new iir-type digital fractional order differentiator, Signal Processing 83 (11) (2003) 2359–2365.

[23] W.-D. Chang, D.-M. Chang, Design of a higher-order digital differentiator using a particle swarm optimization approach, Mechanical Systems and Signal Processing 22 (1) (2008) 233–247.

[24] C.-K. Chen, J.-H. Lee, Design of high-order digital differentiators using l/sub 1/error criteria, IEEE Transactions on Circuits and Systems II: Analog and Digital Signal Processing 42 (4) (1995) 287–291.

[25] A. Sabatini, Real-time kalman filter applied to biomechanical data for state estimation and numerical differentiation, Medical and Biological Engineering and Computing 41 (1) (2003) 2–10.

[26] M. Sharifi, M. Seif, M. Hadi, A comparison between numerical differentiation and kalman filtering for a leo satellite velocity determination, Artificial Satellites 48 (3) (2013) 103–110.

[27] J. Moore, Optimum differentiation using kalman filter theory, Proceedings of the IEEE 56 (5) (1968) 871–871.

[28] V. I. Utkin, Sliding modes in control and optimization, Springer Science & Business Media, 2013.

[29] A. Levant, Robust exact differentiation via sliding mode technique, automatica 34 (3) (1998) 379–384.

[30] W. T. Higgins, A comparison of complementary and kalman filtering, IEEE Transactions on Aerospace and Electronic Systems (3) (1975) 321–325.

[31] L. J. Puglisi, On the velocity and acceleration estimation from discrete time-position signal of linear encoders, Journal of Control Engineering and Applied Informatics 17 (3) (2015) 30–40.

[32] I. Daubechies, The wavelet transform, time-frequency localization and signal analysis, IEEE transactions on information theory 36 (5) (1990) 961–1005.

[33] M. N. Do, M. Vetterli, Texture similarity measurement using kullback-leibler distance on wavelet subbands, in: Image Processing, 2000. Proceedings. 2000 International Conference on, Vol. 3, IEEE, 2000, pp. 730–733.

[34] D. Heric, D. Zazula, Combined edge detection using wavelet transform and signal registration, Image and Vision computing 25 (5) (2007) 652–662.

[35] R. Yan, R. X. Gao, X. Chen, Wavelets for fault diagnosis of rotary machines: A review with applications, Signal processing 96 (2014) 1–15.

[36] T. Abuhamdia, S. Taheri, J. Burns, Laplace wavelet transform theory and applications, Journal of Vibration and Control 0 (0) (2017) 1077546317707103. doi:10.1177/1077546317707103.

[37] L. Ebadi, Z. Helmi, M. Shafri, S. B. Mansor, R. Ashurov, A review of applying second-generation wavelets for noise removal from remote sensing data, Environmental earth sciences 70 (6) (2013) 2679.

[38] M. A. Kabir, C. Shahnaz, Denoising of ecg signals based on noise reduction algorithms in emd and wavelet domains, Biomedical Signal Processing and Control 7 (5) (2012) 481–489.

[39] L. R. Watkins, Review of fringe pattern phase recovery using the 1-d and 2-d continuous wavelet transforms, Optics and Lasers in Engineering 50 (8) (2012) 1015–1022.

[40] T. Abuhamdia, S. Taheri, Wavelets as a tool for systems analysis and control, Journal of Vibration and Control 23 (9) (2017) 1377–1416. doi:10.1177/1077546315620923.

[41] J.-M. Combes, A. Grossmann, P. Tchamitchian, Wavelets: Time-Frequency Methods and Phase Space Proceedings of the International Conference, Marseille, France, December 14–18, 1987, Springer Science & Business Media, 2012.

[42] C. K. Chui, G. Chen, Wavelet kalman filtering, in: Kalman Filtering, Springer, 2017, pp. 171–183.

[43] X. Chen, C. Shen, W.-b. Zhang, M. Tomizuka, Y. Xu, K. Chiu, Novel hybrid of strong tracking kalman filter and wavelet neural network for gps/ins during gps outages, Measurement 46 (10) (2013) 3847–3854.

[44] P. Sun, X. Tang, Y. Huang, G. Sun, Wavelet de-noising kalman filter-based global navigation satellite system carrier tracking in the presence of ionospheric scintillation, IET Radar, Sonar & Navigation 11 (2) (2016) 226–234.

[45] Y. Chen, Q. Zhao, B. Hu, J. Li, H. Jiang, W. Lin, Y. Li, S. Zhou, H. Peng, A method of removing ocular artifacts from eeg using discrete wavelet transform and kalman filtering, in: Bioinformatics and Biomedicine (BIBM), 2016 IEEE International Conference on, IEEE, 2016, pp. 1485–1492.

[46] S. Butterworth, Experimental wireless and the wireless engineer, Wireless Eng 7 (1930) 536.

[47] P. Gaydecki, Foundations of digital signal processing: theory, algorithms and hardware design, Vol. 15, Iet, 2004.

[48] B. Yu, D. Gabriel, L. Noble, K.-N. An, Estimate of the optimum cutoff frequency for the butterworth low-pass digital filter, Journal of Applied Biomechanics 15 (3) (1999) 318–329.

[49] J. H. Challis, A procedure for the automatic determination of filter cutoff frequency for the processing of biomechanical data, Journal of Applied Biomechanics 15 (3) (1999) 303–317.

[50] P. Zarchan, H. Musoff, Fundamentals of Kalman Filtering: A Practical Approach, no. v. 190 in Fundamentals of Kalman filtering: a practical approach, American Institute of Aeronautics and Astronautics, Incorporated, 2000.

[51] M. Euston, P. Coote, R. Mahony, J. Kim, T. Hamel, A complementary filter for attitude estimation of a fixed-wing uav, in: Intelligent Robots and Systems, 2008. IROS 2008. IEEE/RSJ International Conference on, IEEE, 2008, pp. 340–345.

[52] Y. Tian, H. Wei, J. Tan, An adaptive-gain complementary filter for real-time human motion tracking with marg sensors in free-living environments, IEEE Transactions on Neural Systems and Rehabilitation Engineering 21 (2) (2013) 254–264.

[53] R. Kottath, P. Narkhede, V. Kumar, V. Karar, S. Poddar, Multiple model adaptive complementary filter for attitude estimation, Aerospace Science and Technology (2017).

[54] E. Chalmers, J. Le, D. Sukhdeep, J. Watt, J. Andersen, E. Lou, Inertial sensing algorithms for long-term foot angle monitoring for assessment of idiopathic toe-walking, Gait & Posture 39 (1) (2014) 485 – 489.

[55] S. Winder, Chapter 9 - phase-shift networks (all-pass filters), in: S. Winder (Ed.), Analog and Digital Filter Design (Second Edition), second edition Edition, EDN Series for Design Engineers, Newnes, Woburn, 2002, pp. 243 – 284. doi:10.1016/B978-075067547-5/50009-9.

[56] A. Bariska, Time machine, anyone? (Mar. 2008).
URL https://www.dsprelated.com/showarticle/54.php

[57] G. Strang, T. Nguyen, Wavelets and filter banks, SIAM, 1996.

[58] I. Daubechies, Ten lectures on wavelets, vol. 61 of cbms-nsf regional conference series in applied mathematics (1992).